NEOPLASIA
www.neoplasia.com
Volume 11 Number 2 February 2009 pp. 196–206 196

Transcriptional Regulation of Urokinase-type Plasminogen Activator Receptor by Hypoxia-Inducible Factor 1 Is Crucial for Invasion of Pancreatic and Liver Cancer[1]

Peter Büchler*,†, Howard A. Reber†, James S. Tomlinson†, Oliver Hankinson‡, Georgis Kallifatidis§, Helmut Friess*, Ingrid Herr§ and Oscar J. Hines†

*Department of General Surgery, Klinikum rechts der Isar, Technische Universität München, 81675 München, Germany; †Department of Surgery, Geffen School of Medicine at UCLA, UCLA, Los Angeles, CA 90095, USA; ‡Department of Pathology and Laboratory Medicine, Geffen School of Medicine at UCLA, UCLA, Los Angeles, CA 90095, USA; §Department of Surgery, Division of Molecular OncoSurgery, University of Heidelberg, 69221 Heidelberg, Germany

Abstract

Angioinvasion is critical for metastasis with urokinase-type plasminogen activator receptor (uPAR) and tumor hypoxia-activated hypoxia-inducible factor 1 (HIF-1) as key players. Transcriptional control of uPAR expression by HIF has never been reported. The aim of the present study, therefore, was to test whether tumor hypoxia-induced HIF expression may be linked to transcriptional activation of uPAR and dependent angioinvasion. We used human pancreatic cancer cells and a model of parental and derived HIF-1β–deficient mouse liver cancer cell lines and performed Northern blot analysis, nuclear runoff assays, electrophoretic mobility shift assay, polymerase chain reaction–generated deletion mutants, luciferase assays, Matrigel invasion assays, and *in vivo* angioinvasion assays in the chorioallantoic membrane of fertilized chicken eggs. Urokinase-type plasminogen activator receptor promoter analysis resulted in four putative HIF binding sites. Hypoxia strongly induced *de novo* transcription of uPAR mRNA. With sequential deletion mutants of the uPAR promoter, it was possible to identify one HIF binding site causing a nearly 200-fold increase in luciferase activity. Hypoxia enhanced the number of invading tumor cells *in vitro* and *in vivo*. In contrast, HIF-1β–deficient cells failed to upregulate uPAR expression, to activate luciferase activity, and to invade on hypoxia. Taken together, we show for the first time that uPAR is under transcriptional control of HIF and that this is important for hypoxia-induced metastasis.

Neoplasia (2009) 11, 196–206

Introduction

A hypoxic microenvironment of low oxygen is found in solid tumors including pancreatic cancer [1]. It is associated with restrained cell proliferation and it promotes tumor aggressiveness and acquired resistance to treatment [2,3]. The latter occurs as a direct result of reduced generation of free radicals and by the reduction of fixation of radiation-induced DNA damage [1,4]. Clinically, tumor hypoxia occurs heterogeneously within the tumor mass and is independent of tumor size, stage, histologic diagnosis, and tumor grade [5–7]. It has been suggested that hypoxia selects for more malignant cell clones, that is, by promoting those with diminished apoptotic potential owing to p53 alterations [8] or, for example, by activating adenosine A(3) receptor–Akt pathway, which mediates Bad inactivation and favors cell survival [9,10]. Furthermore, hypoxia was shown to select for cell clones with reduced E-cadherin expression and, therefore, promotes tumor cell metastasis [11–13]. Hypoxia also promotes adaptive processes associated with metabolic adaptation, improved systemic oxygen supply, cell survival, and cell proliferation [14].

Hypoxia-inducible factor 1 (HIF) is a transcriptional activator that functions as a master regulator of oxygen homeostasis in all metazoan

Address all correspondence to: Peter Büchler, MD, Klinikum rechts der Isar, Technische Universität München, Department of General Surgery, Ismaninger Strasse 22, 81675 Munich, Germany. E-mail: buechler@chir.med.tu-muenchen.de

[1]This article refers to supplementary materials, which are designated by Figures W1 to W3 and are available online at www.neoplasia.com.

Received 28 June 2008; Revised 29 November 2008; Accepted 1 December 2008

DOI 10.1593/neo.08734

species. It is a heterodimeric protein composed of a constitutively expressed HIF-1β subunit and an oxygen-regulated HIF-1α subunit [15]. Transcriptional activation of HIF-1 and HIF-2 in hypoxia is mediated by the inhibition of asparagine-hydroxylase HIF-1 that in normoxia hydroxylates the HIF-1α C-terminal activation domain, precluding thus interaction with transcriptional coactivators p300/CBP [16–18]. Inhibition of prolyl hydroxylases in hypoxia also affects the stability of HIF-1α [19,20]. One hydroxylated binding of the von Hippel-Lindau (VHL) protein [21] results in ubiquitination and proteasomal degradation [22]. Under hypoxic conditions, the rate of hydroxylation declines, leading to HIF activation and thus providing a mechanism by which changes in oxygenation are transduced to the nucleus as changes in gene expression [23].

Previous studies have demonstrated that HIF transactivates genes involved in energy metabolism, involving glucose transporters and glycolytic enzymes in response to reduced oxygen availability [24]. Other known target genes of HIF play an important role in angiogenesis, erythropoiesis, cell proliferation, and vasomotor responses [14]. Although the role of HIF in angiogenesis is well characterized [25], the function of this transcription factor in uPAR-mediated invasion and metastasis is less clear and not examined in detail [26].

Available data suggest that tumor cells need to migrate across tissue barriers and gain access to systemic circulation to be disseminated to metastatic organs [27]. During this multistep process, tumor cells detach from the primary tumor and invade tumor blood vessels (intravasation) which they finally extravasate to metastasize in organs (extravasation) where they form the secondary lesion. Dissemination occurs through blood or lymphatic circulation breaching of the vasculature wall, and this seems to be the crucial rate-limiting event during metastasis [27,28]. This concept is simple, although it is not known why only some but not all cells of a clonal tumor population acquire the ability to cross tissue borders. Some of the players within the initial scenario of intravasation have been identified, and the predominant protease system, which apparently regulates angioinvasion, seems to involve the system of urokinase-type plasminogen activator (uPA) and its receptor (uPAR) [27,29].

Urokinase-type plasminogen activator receptor is a three-domain (D1-3) glycosyl phosphatidylinositol–anchored cell surface receptor with a high affinity for uPA, pro-uPA, and ATF [30,31]. Urokinase-type plasminogen activator receptor can be released from the plasma membrane by cleavage of the glycosyl phosphatidylinositol anchor and is then found as a soluble molecule (suPAR). Intact uPAR binds uPA with high affinity but can also bind vitronectin and members of the integrin family [32,33]. Bound uPAR is found at focal adhesion sites, yet the cellular mechanisms of signal transduction is unknown [32,34]. So far, at least three transmembrane proteins have been identified to be targeted by uPAR: integrins, G protein–coupled receptors, and caveolin [30,35]. Control of uPAR transcription is located within the first 400 bp upstream of the transcription initiation site driven by a nonspecified TATA-less promoter [36]. Despite recent reports indicating a correlation between hypoxia-induced up-regulation of uPAR and uPA levels and a bad prognosis for patient survival in pancreatic cancer [37], transcriptional regulation of the human uPAR promoter by HIF has never been examined.

In the present study, we identified *uPAR* gene as a novel target gene transcriptionally regulated by HIF. We show that hypoxia regulates tumor cell angioinvasion and metastasis through activation of HIF and transcriptional up-regulation of uPAR, the main mediator in tumor cell invasion. Our data establish a molecular link between the clinical observation of increased tumor aggressiveness and tumor hypoxia in pancreatic and liver cancer cells.

Materials and Methods

Cell Lines

Human pancreatic cell lines AsPc-1, Capan-2, MIA PaCa-2, and PANC-1 were purchased from the American Tissue Type Culture Collection (ATCC, Rockville, MD). Parental mouse hepatoma cells Hepa-1c1c7 and the derived mutant c4 subclone deficient for an obligatory component of the HIF-1 heterodimer, HIF-1β, were described previously [38]. The c4 cell line carries a mutated PAS region of *ARNT* gene, causing impaired hypoxic induction of HIF binding to DNA. Cells were grown at 37°C in Dulbecco's modified Eagle's medium supplemented with 10% heat-inactivated fetal bovine serum, 25 mM HEPES, and 2 mM L-glutamine (Life Technologies Gibco BRL, Karlsruhe, Germany). For experimental hypoxia, cells were subjected to a hypoxic microenvironment induced by flushing a sealed incubator chamber with a gas mixture containing 1% O_2 and 5% CO_2 balanced with nitrogen.

Northern Blot Analysis, Probe Synthesis, and Quantitative Reverse Transcription–Polymerase Chain Reaction

RNA isolation and Northern blot analysis were performed as previously described [3]. For probe synthesis, full-length cDNA clones for uPA and uPAR were purchased from ATCC and amplified in *Escherichia coli* JM109. Recombinant plasmids were isolated, and cDNA inserts were excised and labeled with [α-^{32}P]dCTP (ICN, Irvine, CA) by random priming. Quantitative reverse transcription–polymerase chain reaction has been performed as described elsewhere [39].

Western Blot Analysis

Pancreatic cancer cells were grown on 60-mm dishes. When 60% confluent, cells were incubated in Opti-MEM for 12 hours, followed by 16 hours of hypoxic treatment, washed twice with phosphate-buffered saline before lysis with 2× sodium dodecyl sulfate–polyacrylamide gel electrophoresis (SDS-PAGE) sample buffer (Bio-Rad, Hercules, CA). Protein electrophoresis and transfer to nylon membranes were performed as previously described [40]. Membranes were blocked in 5% nonfat milk in Tris-buffered saline for 1 hour. Membranes were incubated overnight with an anti uPAR-specific antibody (3932; American Diagnostica, Greenwich, CT) at a 1:1000 dilution in Tris-buffered saline and 0.05% Tween 20. The membrane was washed three times with Tris-buffered saline and 0.05% Tween 20 and then incubated with horseradish peroxidase–conjugated antirabbit IgG antibody for 1 hour. Immunoreactive bands were detected by enhanced chemiluminescence. Antibodies specific for ERK1/2 and phospho-ERK were purchased from Cell Signaling (Beverly, MA).

Analysis of Rac1 Activation

Affinity precipitation of active Rac1 was performed using the fusion protein PAK-1 PBD, which binds specifically to the active, GTP-bound forms of Rac1. MIA PaCA-2 and PANC-1 cells were cultured in serum-free medium for 6 hours and exposed to 1.0% O_2 for 16 hours. Control cultures were maintained in 21% O_2. Cell extracts were prepared in ice-cold radioimmunoprecipitation assay buffer containing protease inhibitor cocktail and 1 mM sodium orthovanadate. The extracts were incubated with 20 μg of PAK-1 PBD coupled to glutathione-Sepharose for 60 minutes at 4°C. The glutathione-Sepharose

was washed three times and treated with SDS sample buffer to dissociate the PAK-1 PBD and associated proteins. Cell extracts were subjected to SDS-PAGE, and immunoblot analysis was performed to detect Rac1. Samples of each cell extract were also subjected to immunoblot analysis before incubation with PAK-1 PBD to determine total Rac1, uPAR, and tubulin, as a loading control.

Measurement of Apoptosis and Flow Cytometry

Apoptosis was induced by gemcitabine (kind gift from Eli Lilly, Indianapolis, IN) which was diluted in phosphate-buffered saline (PBS) to a 50-μM stock. Induction of apoptosis was measured by staining of fragmented DNA with Nicoletti buffer and flow cytometry as described [41]. Experiments were performed at least three times in triplicate, and values given are the mean of triplicates ± SD. A total of 2×10^5 cells per sample were used, and at least 1×10^4 cells were counted (FACScalibur and CellQuest Software; Becton Dickinson, San Jose, CA).

Preparation of Nuclear Extracts

Cells were harvested and centrifuged and nuclear extracts were prepared as described previously [42]. The pellet was resuspended in four packed cell volumes of buffer A (10 mM Tris-HCl (pH 7.8), 1.5 mM $MgCl_2$, 10 mM KCl), incubated on ice for 10 minutes, homogenized, and centrifuged at 3,000 rpm for 5 minutes. The pellet was resuspended in three packed cell volumes of buffer C (0.42 M KCl, 20 mM Tris-HCl (pH 7.8), 1.5 mM $MgCl_2$, 20% glycerol) and mixed on a rotator at 4°C for 30 minutes. Nuclear fragments were pelleted for 30 minutes at 14,000 rpm at 4°C. The supernatant was dialyzed once against buffer Z (20 mM Tris-HCl (pH 7.8), 0.1 M KCl, 0.2 mM EDTA, 20% glycerol) for at least 3 hours at 4°C. The lysate was centrifuged for 10 minutes at 14,000 rpm at 4°C and aliquoted.

Electrophoretic Mobility Shift Assay

Oligonucleotide probes were designed based on published human sequences (GenBank Accession No. S78532; Figure W1) for the 5′-region of the *uPAR* gene and purchased from Life Technology (Life Technologies, Gaithersburg, MD). For electrophoretic mobility shift assay (EMSA), an oligonucleotide was chosen, which contained the first putative HIF binding site present within the uPAR promoter (–34 to –39 bp). The binding site–specific sequence (coding strand) of the wild type probe was 5′-AGA AG**A CGT GC**A GGG ACC CC-3′, positions to –45 to –25 bp upstream of the start codon. The sequence of the mutant probe was 5′-AGA AGA TTT GCA GGG ACC CC-3′. Radioactive oligonucleotides were generated by 5′ end labeling using T4 polynucleotide kinase (Amersham Pharmacia Biotech, Piscataway, NJ). Binding reactions were done with 5 mg of nuclear extracts, 0.1 mg of denatured calf thymus DNA, and 1 ng of the radiolabeled probe (10,000 cpm). Supershift experiments were done in the presence of a monoclonal anti–HIF-1α antibody H1a67 (Novus Biologicals, Littleton, CO). Electrophoresis was carried out on a 5% nondenaturing polyacrylamide gel at 185 V in 0.3 × TBE (1 × TBE is 89 mM Tris-HCl, 89 mM boric acid, and 5 mM EDTA) at 4°C. Gels were vacuum dried and autoradiographed.

Nuclear Runoff Assay

To measure hypoxia specific up-regulation uPAR mRNA transcription, we performed nuclear runoff assays as described [43]. After cell lysis in 4 ml of lysis buffer (10 mM Tris (pH 7.4), 10 mM NaCl, 3 mM $MgCl_2$, and 0.5% Nonidet P-40) and centrifugation, the nuclear pellet was resuspended in 200 μl of storage buffer (50 mM Tris (pH 8.3), 5 mM $MgCl_2$, 0.1 mM EDTA, and 40% glycerol) for subsequent analysis. Nuclear runoff assays were initiated by incubating 200 μl of the nuclei with 200 μl of reaction buffer (5 μl of 1 M dithiothreitol, and 2 μl of 100 mM ATP, CTP, GTP, and 10 μl of 10 mCi/ml [^{32}P]UTP) for 30 minutes at 30°C. Subsequently, 40 μl of 1 mg/ml DNase I and 1 ml of high salt buffer (0.5 M NaCl, 50 mM $MgCl_2$, 2 mM $CaCl_2$, 10 mM Tris, pH (7.4)) were added and incubated for 5 minutes at 30°C. After incubating samples for 30 minutes (42°C) with 10 μl of proteinase K in 200 μl of SDS-Tris buffer consisting of 5% SDS, 0.5 M Tris, pH 7.4, and 0.125 M EDTA, nuclear RNA was extracted and adjusted to 5×10^6 cpm/ml. Linearized uPAR cDNA (100 μg) was denatured by incubating samples for 30 minutes (23°C) in 0.2 M NaOH and neutralized with 6× SSC. cDNA (5 μg per sample) was slot blotted onto nylon membranes and UV cross-linked. Membranes were hybridized at 42°C with ^{32}P-labeled RNA samples for 24 hours, washed twice in 2× SSC at 65°C for 30 minutes and incubated for 30 minutes at 37°C with 10 mg/ml RNase A. After rinsing in 2× SSC at 37°C for 1 hour, membranes were exposed at 80°C to Kodak XAR-5 films (Sigma-Aldrich, St. Louis, MO).

uPAR Promoter Activity

All deletion mutants were created by polymerase chain reaction (PCR) using the promoter sequence (GenBank Accession No. S78532) as a template. The constructs were designed to analyze all potential hypoxia response elements (RCGTG) present in the uPAR promoter. The following forward primers, containing an artificial *Kpn* I restriction site, were used: 1 sense (1S) –870 to –849: TTT TTG GCT GAA GTG TCT TTT; 2 sense (2S) –638 to –617: TTT TAA TGT AGG TGC AAT GCC; 3 sense (3S) –523 to –502: GGC ACA GCA GGA AGC AAA GCA. The reverse primers, to which an additional *Bgl* II restriction site was attached were as follows: 1 antisense (1AS) –20 to +1: ACA GGA GCT GCC CTC GCG ACA; 2 antisense (2AS) –77 to –56: ACA AAA CTG CCT CCT TCC TGA; 3 antisense (3AS) –164 to –143: CCC CTC CTC CCG TAC GAA CC. For site-directed mutagenesis of the HRE, the following reverse primer was used –45 to –25: AGA AG**A TTT G**CA GGG ACC CC. The PCR fragments were isolated, digested, and subcloned into the multicloning site upstream of the luc+ reporter gene of the pGL3-Basic vector (Promega Corporation, Madison, WI).

Luciferase Assays

Human pancreatic cancer and murine hepatoma cell lines (1×10^5 cells) were seeded in 60-mm dishes and cultured for 48 hours. Cells were cotransfected with 3 μg of the different luciferase reporter gene constructs along with 1 μg of pRL-CMV-Rluc (Promega). Briefly, the plasmid mixture and 20 μl of Lipofectine reagent were mixed in 200 μl of Opti-MEM (Life Technology, Rockville, MD) for 30 minutes at room temperature and were added to approximately 1×10^5 cells together with 800 μl of Opti-MEM per 35-mm dish. After 6 hours of incubation, 1 ml of cell type–specific medium containing 20% fetal bovine serum was added. At 24 hours after transfection, the cells were either grown under hypoxic or normoxic conditions for additional 12 hours. The cells were washed twice with PBS and harvested in 500 μl of 1 × Passive Lysis Buffer (Promega) followed by the measurement of the firefly and renilla luciferase activities on a Lumat LB 9507 luminometer (Berthold, Bundoora, Australia). The relative firefly luciferase activities were calculated by normalizing transfection efficiency according to the renilla luciferase activities. Fold activation of luciferase activity was calculated relative

to control cells that were given the reference value of 1 as described [44]. The experiments were performed in triplicate, and similar results were obtained from independent experiments.

In Vitro *Invasion Assay and uPAR RNA Interference*

The effect of hypoxia on the invasive potential of pancreatic cancer cells was tested in a Costar Transwell system with inserts containing a polycarbonate membrane with 8-mm pores (Corning Costar, Corning, NY). Matrigel in serum-free medium (Matrigel; Collaborative Biomedical Products, Bedford, MA) served as substrate for invasion. Briefly, the Transwell invasion chambers were coated with 100 ml of a 1.0-mg/ml solution of Matrigel diluted in cold Dulbecco's modified Eagle's medium and allowed to air dry for 12 hours. A total of 5×10^4 MIA PaCa-2 cells dissolved in 100 ml of serum-free medium were added to the upper well of the invasion chamber. The assay was done in triplicates. Cells were either cultured under normoxic conditions or subjected to a hypoxic microenvironment, both in the presence and in the absence of 15 mg/ml blocking anti-uPAR antibody 3936 (American Diagnostica). After 24 hours, cells that invaded through the Matrigel-coated membrane were fixed in Carnoy's fixative (25% acetic acid, 75% methanol) for 10 minutes and stained for 3 hours in 1% toluidine blue, 1% sodium borate). After several washes in tap water, the membranes were removed with a scalpel blade and analyzed on a microscopic slide. The invasive index was determined by evaluating the total number of stained cells at the underside of the polycarbonate membranes under a microscope. For recombinant uPAR overexpression, cells were transfected with a uPAR cDNA expression plasmid (pEGFP-N1) or empty vector using Lipofectamine (Invitrogen, Karlsruhe, Germany) and grown in a selection medium (1200 μg/ml G418; Promega, Mannheim, Germany). The uPAR-RNAi vector was also based on the pEGFP-N1 backbone. The uPAR sequence from +77 to +98 was used as the target sequence, and for convenience, a self-complimentary oligonucleotide was used. The uPAR sequence was 21 bases in length with a 9-base loop region and *Bam*HI sites incorporated at the ends (gatcctacagcagtggagagcgattatataataatcgctctccactgctgtag). The oligonucleotide was self-annealed in 6× SSC buffer and ligated onto the *Bam*HI site of a linearized pEGFP-N1 vector plasmid. The orientation of the insert was not relevant because the oligonucleotides were self-complimentary. Bovine growth hormone poly-A terminator served as a stop signal for RNA synthesis for all constructs. Moreover, for uPAR knock-down experiments, pancreatic cancer cells were transfected with siRNA (uPAR siRNA, sc-36781; Santa Cruz Biotechnology, Heidelberg, Germany) according to the manufacturer's instructions. As control, a scrambled sequence siRNA was used (Santa Cruz Biotechnology), which specifically targets a sequence of human uPAR cDNA (5′-GGTGAAGAAGGGCGTCCAA-3′), and a nonsilencing siRNA (5′-AACCTGCGGGAAGAAGTGG-3′) was used as a control. Suppression of uPAR protein was confirmed by Western blot analysis.

In Vivo *Intravasation and Metastasis Assays*

For intravasation, invasion, and metastasis assays *in vivo*, COFAL-negative fertilized eggs from specific pathogen-free avian supply (SPAFAS, Norwich, CT) were used and maintained at 37°C in a humidified incubator for 8 days. Tumor cells, 75% confluent, were detached from the cell culture dish with cell dissociation solution (Sigma), washed, and resuspended in PBS. Usually, 5×10^5 cells were inoculated onto a chorioallantoic membrane (CAM; so-called upper CAM) of a 9-day-old chick embryo, in which an artificial air sac was created. For intravasation assays, the CAM opposite to the inoculated tumor cells was removed and immediately subjected to lysis buffer or frozen in liquid nitrogen and stored at −80°C for further analysis.

For uPAR inhibition, 40 mg/ml neutralizing uPAR antibody 3936 (American Diagnostica), or for controls, an isotype-matched mouse–antihuman γ-tubulin antidody (sc-17788; Santa Cruz Biotechnology), was added ontopically on the CAM.

DNA Extraction and Human Alu PCR Amplification

Frozen tissue was homogenized in liquid nitrogen. Genomic DNA was isolated using a DNA extraction kit (Gentra Systems, Minneapolis, MN). Specific primers for a highly conserved human Alu sequence are as follows: Alu-sense, 5′- ACG CCT GTA ATC CCA GCA CTT-3′; and Alu antisense, 5′- TCG CCC AGG CTG GAG TGC A-3′, which produced a band of 224 bp [27]. Polymerase chain reaction was performed as described [27].

Statistical Analysis

Experiments were repeated at least three times. Results are expressed as means ± SE. Statistical significance was determined by Student's *t* test and Fisher's exact test. $P < .05$ was considered to be statistically significant.

Results

Hypoxia Induces Transcription of uPAR

Regulation of uPAR mRNA expression was tested in AsPC-1, Capan-2, MIA PaCa-2, and PANC-1 cells. In addition, the mouse hepatoma cell line Hepa-1c1c7 and its HIF-1β–deficient mutant c4 subclone were used to analyze whether up-regulation of uPAR mRNA is due to HIF activation [38]. Culturing the cells for 4, 8, 12, and 24 hours under hypoxic conditions resulted in a gradual increase of uPAR mRNA in each cell line as examined by Northern and Western Blot analyses (Figure 1*A*). Whereas Hepa-1c1c7 cells strongly upregulated uPAR expression on hypoxic exposure, HIF-1–deficient cells c4 showed only minimal activation as expected (Figure 1, *A* and *B*). Basal expression of uPAR mRNA was highest in the undifferentiated cell line AsPC-1 and decreased proportionately to the differentiation grade of the pancreatic cancer cells. The uPA mRNA levels remained unchanged by hypoxia (data not shown). To demonstrate functional activity of uPAR signaling in pancreatic cancer cells, we analyzed the presence of endogenous ligands for uPAR (Figure 1*C*). First, we examined the basal level of activation of ERK/MAPK and Rac1 in MIA PaCA-2 and PANC-1 cells that were transferred for 16 hours to 1.0% O_2. Both signaling proteins were activated under hypoxic conditions (Figure 1*C*). Because aggressiveness of pancreatic carcinoma cell lines is exemplified by resistance to gemcitabine standard chemotherapy, the percentage of apoptosis induction correlated to the differentiation grade except for Capan-2 cells, thus paralleling the findings for uPAR mRNA up-regulation (Figure 1*D*).

Because hypoxia is known to inhibit Cap-dependent transcription, which causes stabilization of mRNA transcripts, we determined whether the observed up-regulation of uPAR mRNA transcripts is due to increased transcription or rather accumulation of mRNA [45,46]. A nuclear runoff transcription assay was performed and evaluated by densitometry. Cells were cultured for 16 hours under hypoxic or normoxic conditions. Whereas uPAR mRNA transcription increased in all pancreatic cancer cell lines and parental hepatoma cells, the mutant c4 subclone failed to upregulate uPAR transcription,

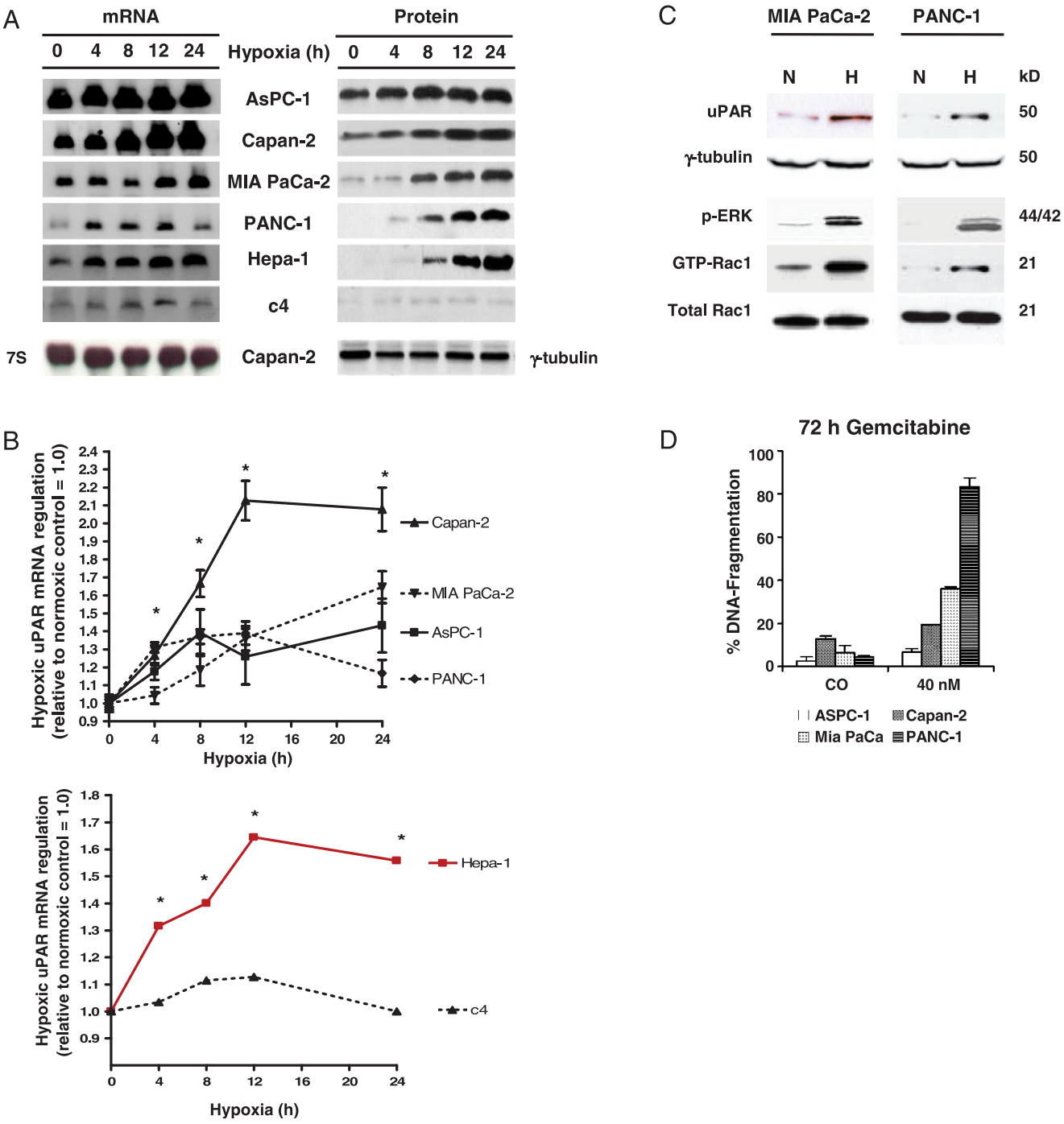

Figure 1. (A) Hypoxia enhances uPAR expression in Northern blot and Western blot experiments. Human pancreatic cancer cell lines AsPC-1, Capan-2, MIA PaCa-2, and PANC-1 together with the murine hepatoma cell line Hepa-1c1c7 and its mutated cell clone c4, lacking functional HIF-1β, were cultured under normoxic or hypoxic conditions. After 24 hours, total RNA and protein were isolated, size-fractionated, and transferred to membranes, which were hybridized in Northern blot experiments with a cDNA probe containing 500 bp of the human *uPAR* gene or in Western blot experiments with uPAR antibody 3932. The 7 S and γ-tubulin probes served as controls to demonstrate equal loading. (B) Densitometry of hypoxia-induced uPAR expression was done as described in the Materials and Methods section. The signal intensity of untreated normoxic control cells was measured and defined as a relative optical density of 1.0. On the basis of the individual signal intensity, the increase or the decrease of the relative optical density in comparison with untreated normoxic cells was determined. *$P < .05$. (C) Cell signaling factors known to be downstream of uPAR were analyzed. MIA PaCa-2 and PANC-1 cells were cultured for 16 hours in 21% O_2 (N) or 1.0% O_2 (H). Cell extracts were affinity-precipitated and subjected to immunoblot analysis to detect GTP-bound Rac1. The original cell extracts were studied by immunoblot analysis to determine total Rac1. Cell extracts were also probed for phosphorylated ERK/MAPK and uPAR. (D) DNA fragmentation assay. AsPC-1, Capan-2, MIA PaCa-2, and PANC-1 were incubated with 40 nM gemcitabine, and 72 hours later, apoptosis was determined by Nicoletti staining of fragmented DNA and FACS analysis.

as expected (Figure 2, *A* and *B*). Addition of actinomycin D (5 μg/ml), which binds to DNA and inhibits RNA synthesis, resulted in a complete suppression of transcriptional activity as analyzed in MIA PaCa-2 cells (Figure 2*C*). mRNA kinetic analysis such as determination of uPAR mRNA half-life in normoxia and in hypoxia did not result in a different half-life (Figure 2*B*). Thus, hypoxia does not seem to affect the stability of uPAR mRNA, suggesting that the observed increase in uPAR mRNA levels by hypoxia was due to an increase in transcription for the uPAR promoter.

HIF Regulates uPAR Promoter Activity

Sequence analysis of the human uPAR promoter (GenBank Accession No. S78532) revealed four putative binding sites for HIF. Sequence analysis was done for the consensus HRE sequences (5′-RCGTG-3′) [23] and the HRE motifs 5′-BACGTSSK-3′ (B = G/C/T, S = G/C, and K = G/T) [47,48]. The first potential HIF binding site, HRE-1 at position −34 to −39, the second site HRE-2 at position −98 to −102, and the third binding site, HRE-3 at position −547 to −552, were identified on the sense strand. The fourth binding site, HRE-4 at position −786 to −790, was located on the antisense strand (Figure W1). To test whether the identified HRE sequences within the HIF promoter contribute to regulation, we generated a series of deletion mutants, which were fused to the luciferase reporter gene of the pGL3 basic vector (Figure 3*A*). MIA PaCa-2 cells were transfected with the PC 1.1, PC 2.2, PC 3.3, PC 1.3, PC 3.1, or PC 3.2 constructs. After 36 hours, cells were exposed to hypoxia, and luciferase assays were performed after additional 12 hours (Figure 3*B*). The wild type construct PC 1.1 and the mutant construct PC 3.1 containing HRE-1 and HRE-2 showed an almost 200-fold induction of luciferase activity. In contrast, deletion of consensus HRE-1 in PC 2.2, PC 3.3, PC 1.3, and PC 3.2 led to an almost complete down-regulation of promoter activity except of PC 2.2. These minimal active construct still contains functional HRE-3 and HRE-2 sites conferring a rest-activity of 44-fold. Because neither HRE-2 alone in PC 3.2 nor HRE-3 alone in PC 1.3 showed activity, the rest induction in PC 2.2 might be due to surrounding sequences.

To clearly demonstrate that HRE-1 is most important for hypoxia-induced activation of the uPAR promoter, we generated two additional promoter constructs. In the PC 3.MUT construct, the putative HIF binding site was mutated to ATTTG, the same mutation already assayed by EMSA. The corresponding wild type construct is PC 3.1. In MIA PaCa-2 cells, the wild type PC 3.WT construct showed a nearly 200-fold increase in reporter gene activity; whereas the mutated construct PC 3.MUT was reduced to a 2.9-fold induction in reporter gene activity (Figure 3*C*). To further investigate the role of hypoxic induction of HIF, we transfected the Hepa-1c1c7 parental and its derived HIF-1β–deficient subclone c4 with the PC3.1 vectors as well. Whereas the parental cell line strongly upregulates transcription from the uPAR promoter (approximately 130-fold, $P < .01$), the mutant c4 cells exhibited only a slight increase (approximately 20-fold) in the transcriptional rate, as expected, because HIF-binding activity is blocked.

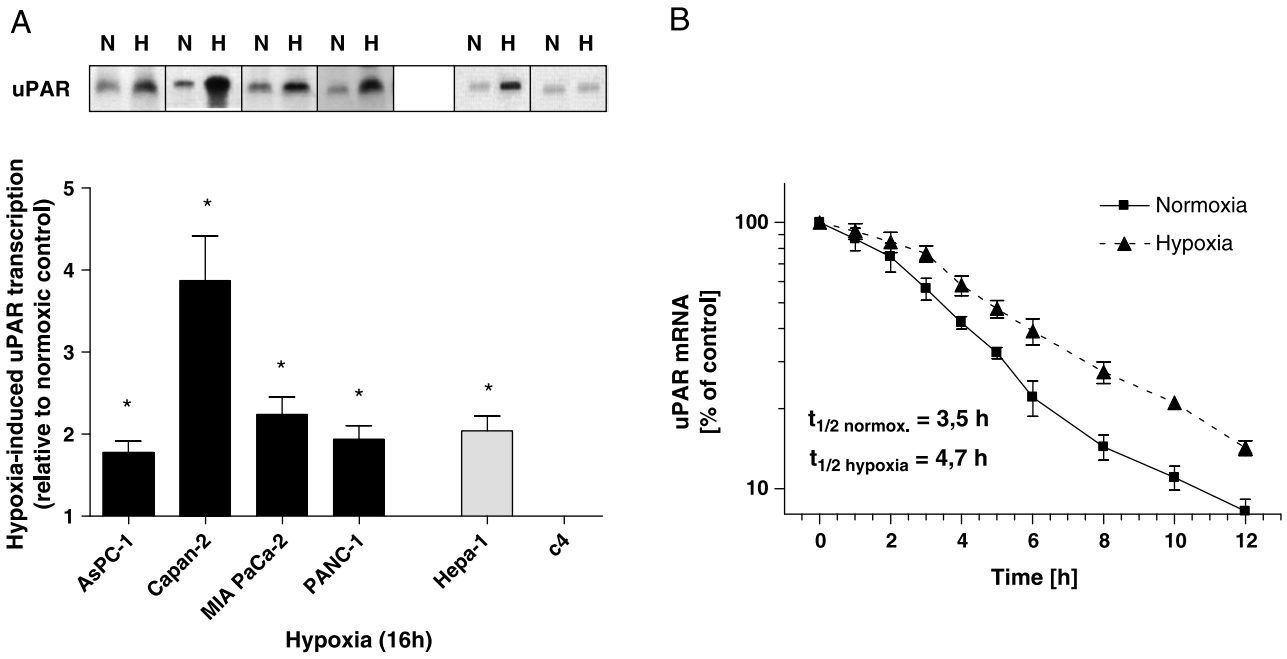

Figure 2. Hypoxia enhances uPAR transcription. (A) Top panel: Nuclear runoff assays comparing normoxic (N) and hypoxic (H) uPAR transcription. Immediately after reaching 80% confluence, cells were exposed to normoxia or hypoxia for 16 hours, and nuclei were prepared. [α-^{32}P]UTP was incorporated in total RNA by *in vitro* transcription assays as described in the Materials and Methods section. The radioactive-labeled RNA samples were hybridized to cDNA specific for uPAR, and autoradiography was performed. Lower panel: The signal intensity of normoxic control cells was defined as a relative optical density of 1.0. On the basis of the individual signal intensity, the increase or the decrease of the relative optical density in comparison with untreated normoxic cells was determined. *$P <$ .05. (B) Effect of hypoxia on mRNA stability in MIA PaCa-2 cells. RNA was isolated from cells cultured under normoxic and hypoxic conditions after incubating with actinomycin D (5 mg/μl) for the indicated time. Quantitative reverse transcription–polymerase chain reaction was performed and uPAR mRNA-quantified. Values of control cells were set at 100%. Each graph represents mean ± SEM for three independent experiments.

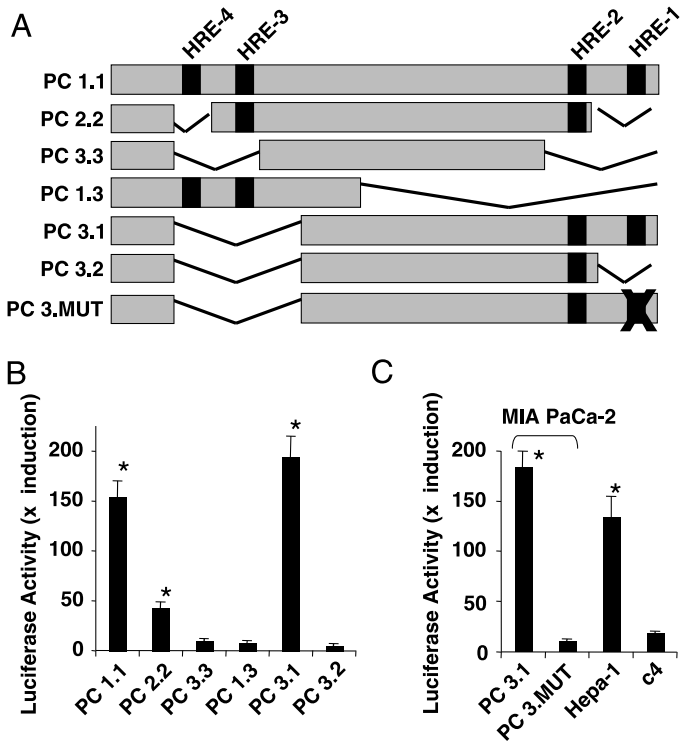

Figure 3. The consensus HRE within the uPAR promoter regulates hypoxia-induced promoter activity. (A) Scheme of the human uPAR promoter including putative consensus HREs. The black bars mark putative HREs relative to the ATG codon. A series of deletion mutants were constructed, and the length of the constructs relative to the transcription start site is indicated. (B) MIA PaCA-2 cells were transfected as described in the Materials and Methods section. Transfected cells were maintained at 21°C and 1% O_2 for 16 hours. Luciferase reporter gene assays were performed, and luciferase activities were normalized by using a dual-luciferase reporter system, in which relative firefly luciferase activities were calculated thus normalizing transfection efficiency according to the renilla luciferase activities. Values represent means ± SD of $n = 3$ experiments performed in duplicate. Statistical differences are indicated by asterisks (*$P < .05$, Student's paired t test). (C) MIA PaCa-2, Hepa-1, and c4 cells were transfected with the constructs indicated and analyzed as described above.

DNA-binding activity of HIF was tested by using a synthetic oligonucleotide corresponding to the consensus HRE-1 at –34 to –39 bp within the uPAR promoter by EMSA. Hypoxia-inducible factor 1–binding activity was detectable as early as 1 hour after exposure of MIA PaCa-2 cells to hypoxia and increased during the next 4 hours (Figure 4). A supershift obtained by coincubation of monoclonal anti–HIF-1α antibody and absence of binding activity on a 30-fold excess of unlabeled wild type or labeled mutant oligonucleotide demonstrates specificity of HIF-1 binding. Specificity is further underscored by a 30-fold excess of unlabeled mutated oligonucleotide for nonspecific competition, which did not cause any difference in signal intensity.

Hypoxia Increases the Invasive Phenotype But Reduces Cell Division In Vitro

Because uPAR might contribute to tumor invasion and metastasis, we determined the role of hypoxia-mediated uPAR promoter activation on these processes using the Matrigel invasion assay. Pancreatic cancer and hepatoma cells were added to the upper well of the invasion chamber. After an initial growth period of 24 hours, the cells were either cultured under normoxic conditions or subjected to a hypoxic microenvironment, both in the presence and in the absence of blocking anti-uPAR antibody (Figure 5, *A–D*). After 24 hours, the cell fraction that invaded through the Matrigel-coated membrane was fixed, stained, and analyzed by microscopy (Figure 5, *A–D*). In general, the number of cells was lower in cell cultures of hypoxic conditions when compared with cells cultured under normal oxygen levels. However, the ratio of tumor cells crossing the Matrigel-coated basement membrane was significantly higher under conditions of low oxygen levels when compared with the invasiveness under normoxic conditions. Upon addition of the neutralizing anti-uPAR antibody, a strong reduction of tumor cell invasion was seen under both normoxic and hypoxic culture conditions (Figure 5*A*). Urokinase-type plasminogen activator receptor knock-down in a stably transfected

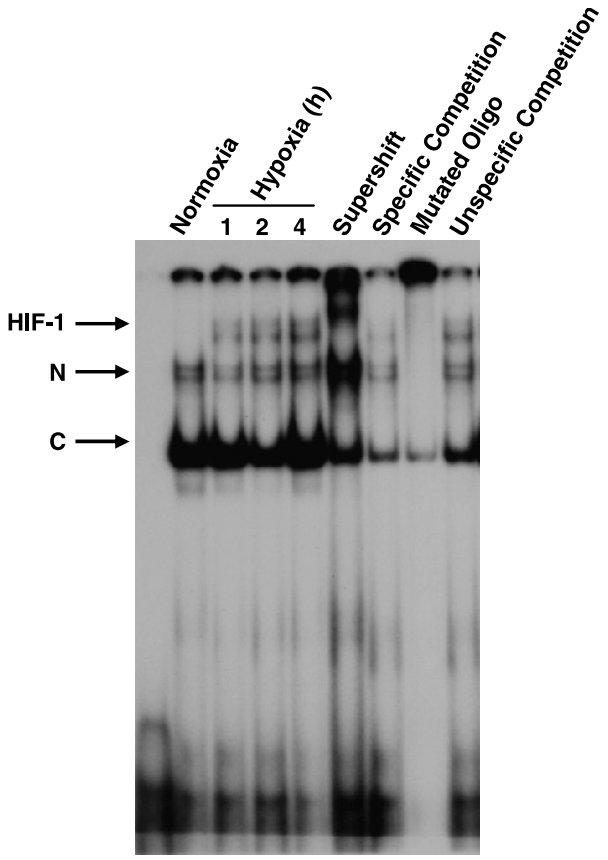

Figure 4. Hypoxia-inducible factor binds to the consensus HRE in uPAR promoter on hypoxia. MIA PaCa-2 cells were cultured under normoxia or hypoxia for 1, 2, and 4 hours. Nuclear proteins were harvested, and binding of a consensus HRE oligonucleotide of the uPAR promoter was analyzed by EMSA as described in the Materials and Methods section. Control experiments were performed with nuclear extracts from cells exposed 4 hours to normoxia or 1, 2, and 4 hours to hypoxia. For supershift and competition experiments, the extract from cells cultured for 4 hours under hypoxic conditions was used. The following reagents were added: anti–HIF-1α antibody (Supershift), a 30-fold excess of unlabeled consensus HRE oligonucleotide of the uPAR promoter (Specific Competition), a labeled mutant consensus HRE oligonucleotide of the uPAR promoter (Mutated Oligo), and a 30-fold excess of unlabeled mutant consensus HRE oligonucleotide of the uPAR promoter. *C* indicates constitutive; *HIF-1*, induced; *N*, nonspecific.

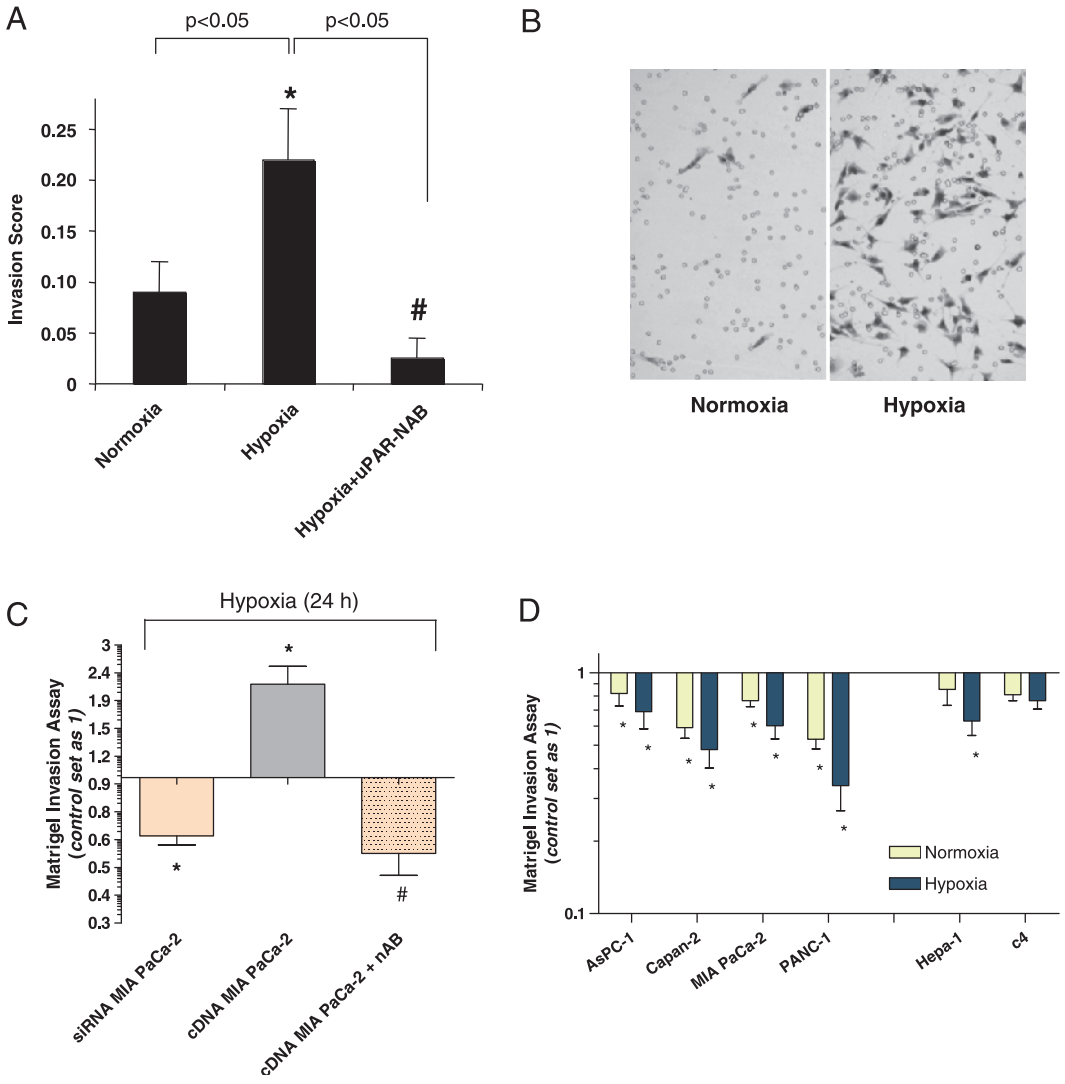

Figure 5. uPAR inhibition reduces tumor cell invasion. (A) MIA PaCa-2 cells were cultured under normoxic or hypoxic conditions as indicated. Invasion was measured by using a reconstituted basement membrane in Costar Transwell inserts containing a polycarbonate membrane with 8-mm pores in the presence of Matrigel as described in the Materials and Methods section. At 24 hours after incubation, cells invading through the semipermeable membrane in the presence or absence of blocking anti-uPAR antibody (uPAR-NAB) were fixed and stained. The invasion score was then determined by counting the total number of stained cells at the underside of the polycarbonate membranes under a microscope. Error bars, SEM across three experiments. (B) An example of the underside of a membrane showing invading cells by light microscopy is displayed for cells treated with normoxia or hypoxia as indicated. (C) Stably transfected MIA PaCa-2 cells expressing uPAR-siRNA or uPAR full-length cDNA were also cultured 24 hours under low oxygen levels. Clearly, the uPAR expression was associated with tumor cell invasion. Overexpression of uPAR could be reverted by the addition uPAR-NAB. (D) siRNA treatment reduced tumor cell invasion in all cell lines both under normoxic and hypoxic culture conditions. For control treatment, a scrambled siRNA oligonucleotide was used. Values represent means ± SD of $n = 3$ experiments performed in duplicate (*$P < .05$, Student's paired t test; $^{\#}P < .05$ compared with hypoxia [A] or uPAR overexpression [D]).

MIA PaCa-2 cell clone also caused a decrease in tumor cell invasion, whereas up-regulation of uPAR let to an increase in invasiveness under conditions of low oxygen (Figure 5*C*). Furthermore, siRNA-based uPAR knock-down experiments resulted in reduced tumor cell invasion under both normoxic and hypoxic culture conditions, when compared with control treated cells (Figure 5*D*).

Angioinvasive Potential In Vivo *Depends on Functional uPAR*

Invasion of blood vessels is the first and rate-limiting process within the metastatic cascade, and uPAR activity may be a critical component. Therefore, we tested the angioinvasive potential of pancreatic cancer cell lines under normoxic and hypoxic conditions in the presence or absence of a neutralizing uPAR antibody in the CAM assay using fertilized chicken eggs. AsPC-1, Capan-2, MIA PaCa-2, PANC-1, Hepa-1c1c7, and c4 cells were inoculated on the CAM of 9-day-old chick embryos. For detecting intravasation, genomic DNA from the opposite CAM was examined for the expression of human Alu sequences by PCR (Figure 6*A*). Angioinvasion was seen under normoxic conditions in all cell lines examined, which could be strongly increased by hypoxia. We further analyzed whether experimental induction of HIF might change the angioinvasive potential. Because induction of hypoxia with cycloheximide was lethal for most chicken eggs, we applied intermittent hypoxia ontopically by flushing the upper CAM with an anoxic gas mixture for 60 minutes every 4 hours.

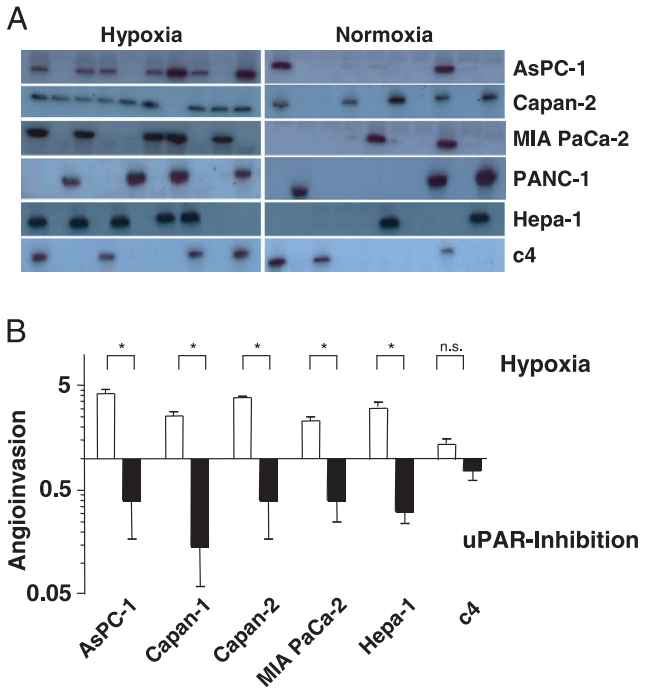

Figure 6. uPAR inhibition blocks angioinvasion after hypoxia *in vivo*. (A) Cells were inoculated onto the dropped CAMs of chicken embryos. Three days later, the lower CAMs were excised, genomic DNA was isolated, and 1 μg of DNA was used to amplify human Alu sequences in the presence of [^{32}P]-dCTP. Polymerase chain reaction products were analyzed by PAGE and visualized by autoradiography. (B) Inhibition of intravasation by a neutralizing uPAR antibody. Inoculated tumor cells were repeatedly flushed with an anoxic gas mixture for the induction of hypoxia. For uPAR inhibition, 40 mg/ml neutralizing uPAR antibody was added ontopically (Materials and Methods section). Alu sequences were analyzed as described above. All experiments were repeated at least three times with 10 eggs in each group. Angioinvasion was calculated relative to normal untreated cells, which were set as 1. *$P < .05$, compared hypoxia *versus* normoxia as well as hypoxia *versus* uPAR inhibition.

This treatment led to increased angioinvasion in chicken eggs (Figures W2 and W3). To further elucidate whether angioinvasion was due to up-regulation of uPAR activity, we ontopically added a neutralizing uPAR antibody resulting in reverted blood vessel invasion below the values of untreated cells (Figure 6*B*), whereas addition of an isotype-matched control antibody did not affect tumor cell invasion (data not shown). Therefore, these data clearly demonstrate involvement of HIF in uPAR-mediated angioinvasion.

Discussion

Hypoxia is considered as a physiological condition in growth of human solid tumors, and the protease systems of uPA/uPAR and metalloproteinases were previously shown to participate in metastatic disease progression. More recent studies suggest that concomitant expression of uPA and uPAR is indispensable for tumor intravasation [27], including our own data demonstrating that hypoxia induces HIF expression in experimental pancreatic cancer [49] and in tumors of patients [3]. These data may be important for future therapeutic approaches because local invasion and early metastatic tumor progression are still the most challenging clinical features of pancreatic cancer. Our present study provides the link by which hypoxia most likely increases local aggressiveness and systemic tumor dissemination. Using established human pancreatic cancer cell lines, we found that the basal expression of uPAR under normoxic conditions was highest in undifferentiated, therapy-resistant cells and could be further induced by hypoxia. These data may correspond to the fact that undifferentiated tumor cells exhibit a more aggressive phenotype and metastasize more frequently when uPAR is upregulated [5,50,51]. Our studies provide evidence that uPAR mRNA expression is only induced in cells carrying functional HIF but not in cells deficient in HIF, as we conclude from a parental and a derived HIF-deficient subclone of a hepatocellular carcinoma [52,53], which failed to upregulate uPAR in response to low oxygen levels. These results are in line with a recent report describing increased expression of uPAR on hypoxia in breast cancer cells, although the underlying mechanisms were not provided [54]. The observed hypoxia-induced activation of uPAR is not due to mRNA stabilization but to enhanced transcription, as we found in nuclear runoff assays. Thus, this finding strengthens our hypothesis that expression of the *uPAR* gene is controlled by HIF.

Despite significant progress has been made in cancer biology, only little is known why some cancer cells do metastasize while others do not, even so these cell populations likely descended from an identical pool of transformed cells [55,56]. One hypothesis is that a specific transient regional tumor microenvironment of low oxygen induces a distinctive epigenetic gene expression profile in a subset of cells, which likely causes selection of more aggressive cell clones [14,51,57–59]. A direct link between hypoxia-induced HIF and regulation of uPAR has never been shown. All we know so far is that the protease systems of uPA/uPAR and metalloproteinases participate in the metastatic disease progression, which is dependent on hypoxia. More recent studies suggest that concomitant expression of uPA and uPAR is indispensable for tumor intravasation [27]. Despite these alarming reports reflecting an important function of uPAR in metastasis, regulation of the promoter region in a hypoxic tumor microenvironment is only marginally understood. Therefore, we created uPAR promoter fragments and confirmed by reporter assays that indeed high induction of uPAR on hypoxia is strictly dependent on the presence of wild type HREs with maximal transcriptional regulatory activity localized at the first HRE closely upstream to the ATG start codon. Our observation is accordant to results of Soravia et al. [36], which found the highest basal transcriptional activity of the uPAR promoter within the first −181 bp upstream of the transcription initiation site. Our analysis of the promoter region of the human *uPAR* gene revealed four potential HREs (RCGTG) within the first 1000 bp upstream to the ATG start codon. Two HREs (ACGTG) were in 5′–3′ orientation, whereas the other two were either TCGTG or oriented in 3′–5′ direction. We deleted all putative HREs alone or in combination by PCR mutagenesis, cloned them in front of a luciferase reporter gene, and tested transcriptional activity of the constructs. By this way, it became apparent that the HRE at position −35 to −39 bp is the main regulatory HRE sequence, and its mutation silenced the transcriptional activity even so some transcriptional activity was detectable in deletion mutants not carrying this HRE (−35/−39 bp). Therefore, we conclude that regulation of the *uPAR* gene expression is under the control of the HRE positioned closely upstream of the translation initiation site.

The importance of uPAR expression in metastasis was further tested using the CAM assay of fertilized chick embryos, which was used to study whether any of these observations had an *in vivo* relevance

for tumor biology. Because it has been suggested that the rate-limiting step for metastasis is angioinvasion and that this process is critically dependent on uPAR expression, we inoculated various pancreatic cancer cell lines, parental HEP1a1c cells as well as its mutant clone c4. Inhibition experiments were performed with a neutralizing uPAR antibody. The angioinvasive potential was found to be highly dependent on uPAR expression. Intermittent hypoxia increased angioinvasion in most cell lines but not in the HIF-deficient c4 cells. Furthermore, addition of a neutralizing anti-uPAR antibody suppressed the angioinvasive phenotype below the levels of normoxic cultures. It is noteworthy that well-differentiated cell lines with low constitutive uPAR expression hardly invaded in chicken blood vessels, whereas low differentiated cell lines expressing higher uPAR levels exhibited a higher constitutive angioinvasive potential corresponding to the finding that undifferentiated tumor cells exhibit a more aggressive phenotype and metastasize more frequently [5]. In line with our results, siRNA toward HIF has been shown to block invasion of a colon carcinoma cell line using *in vitro* Matrigel assays [26].

The functional relevance of uPAR signaling has to be analyzed in the context of its two principal ligands, uPA and its inhibitor plasminogen activator inhibitor 1 (PAI-1). PAI-1 has been shown to be regulated by HIF-1 as well with an up-regulation under hypoxic conditions similar to the up-regulation of uPAR [18,47,60,61]. Thus, HIF-1 may act as a "Janus-faced" or "bicephalous" transcription factor, which regulates both proinvasive and anti-invasive proteins. This is in line with the finding that HIF-1 may promote proapoptotic and antiapoptotic molecules as well, suggesting a potential to regulate cell growth bidirectionally [62–64]. This HIF may differentially activate its target genes dependent on the specific cell type or organ [62,64].

In summary, our studies demonstrate that hypoxic uPAR mRNA expression is under the control of the transcription factor HIF and highly suggest that exposure of pancreatic cancer cells to low oxygen levels increases the angioinvasive phenotype by regulating uPAR expression. This axis defines a master regulator of hypoxic tumor cell invasion and may be important for future therapeutic concepts.

References

[1] Brown JM and Giaccia AJ (1998). The unique physiology of solid tumors: opportunities (and problems) for cancer therapy. *Cancer Res* **58**, 1408–1416.

[2] Hoffmann AC, Mori R, Vallbohmer D, Brabender J, Klein E, Drebber U, Baldus SE, Cooc J, Azuma M, Metzger R, et al. (2008). High expression of HIF1a is a predictor of clinical outcome in patients with pancreatic ductal adenocarcinomas and correlated to PDGFA, VEGF, and bFGF. *Neoplasia* **10**, 674–679.

[3] Buchler P, Reber HA, Buchler M, Shrinkante S, Buchler MW, Friess H, Semenza GL, and Hines OJ (2003). Hypoxia-inducible factor 1 regulates vascular endothelial growth factor expression in human pancreatic cancer. *Pancreas* **26**, 56–64.

[4] Zhao D, Ran S, Constantinescu A, Hahn EW, and Mason RP (2003). Tumor oxygen dynamics: correlation of *in vivo* MRI with histological findings. *Neoplasia* **5**, 308–318.

[5] Helmlinger G, Yuan F, Dellian M, and Jain RK (1997). Interstitial pH and Po_2 gradients in solid tumors *in vivo*: high-resolution measurements reveal a lack of correlation. *Nat Med* **3**, 177–182.

[6] Robey IF, Stephen RM, Brown KS, Baggett BK, Gatenby RA, and Gillies RJ (2008). Regulation of the Warburg effect in early-passage breast cancer cells. *Neoplasia* **10**, 745–756.

[7] Gillies RJ, Schornack PA, Secomb TW, and Raghunand N (1999). Causes and effects of heterogeneous perfusion in tumors. *Neoplasia* **1**, 197–207.

[8] Graeber TG, Osmanian C, Jacks T, Housman DE, Koch CJ, Lowe SW, and Giaccia AJ (1996). Hypoxia-mediated selection of cells with diminished apoptotic potential in solid tumours. *Nature* **379**, 88–91.

[9] Merighi S, Benini A, Mirandola P, Gessi S, Varani K, Leung E, Maclennan S, Baraldi PG, and Borea PA (2007). Hypoxia inhibits paclitaxel-induced apoptosis through adenosine-mediated phosphorylation of bad in glioblastoma cells. *Mol Pharmacol* **72**, 162–172.

[10] Merighi S, Benini A, Mirandola P, Gessi S, Varani K, Leung E, Maclennan S, Baraldi PG, and Borea PA (2005). A3 adenosine receptors modulate hypoxia-inducible factor-1alpha expression in human A375 melanoma cells. *Neoplasia* **7**, 894–903.

[11] Brown JM (1990). Tumor hypoxia, drug resistance, and metastases. *J Natl Cancer Inst* **82**, 338–339.

[12] Browder T, Folkman J, Hahnfeldt P, Heymach J, Hlatky L, Kieran M, and Rogers MS (2002). Antiangiogenic therapy and p53. *Science* **297**, 471.

[13] Beavon IR (1999). Regulation of E-cadherin: does hypoxia initiate the metastatic cascade? *Mol Pathol* **52**, 179–188.

[14] Semenza GL (2003). Targeting HIF-1 for cancer therapy. *Nat Rev Cancer* **3**, 721–732.

[15] Wang GL, Jiang BH, Rue EA, and Semenza GL (1995). Hypoxia-inducible factor 1 is a basic-helix-loop-helix-PAS heterodimer regulated by cellular O_2 tension. *Proc Natl Acad Sci USA* **92**, 5510–5514.

[16] Metzen E and Ratcliffe PJ (2004). HIF hydroxylation and cellular oxygen sensing. *Biol Chem* **385**, 223–230.

[17] Lancaster DE, McNeill LA, McDonough MA, Aplin RT, Hewitson KS, Pugh CW, Ratcliffe PJ, and Schofield CJ (2004). Disruption of dimerization and substrate phosphorylation inhibit factor inhibiting hypoxia-inducible factor (FIH) activity. *Biochem J* **383**, 429–437.

[18] Dayan F, Roux D, Brahimi-Horn MC, Pouyssegur J, and Mazure NM (2006). The oxygen sensor factor-inhibiting hypoxia-inducible factor-1 controls expression of distinct genes through the bifunctional transcriptional character of hypoxia-inducible factor-1alpha. *Cancer Res* **66**, 3688–3698.

[19] Ivan M, Kondo K, Yang H, Kim W, Valiando J, Ohh M, Salic A, Asara JM, Lane WS, and Kaelin WG Jr (2001). HIFalpha targeted for VHL-mediated destruction by proline hydroxylation: implications for O_2 sensing. *Science* **292**, 464–468.

[20] Jaakkola P, Mole DR, Tian YM, Wilson MI, Gielbert J, Gaskell SJ, Kriegsheim A, Hebestreit HF, Mukherji M, Schofield CJ, et al. (2001). Targeting of HIF-alpha to the von Hippel-Lindau ubiquitylation complex by O_2-regulated prolyl hydroxylation. *Science* **292**, 468–472.

[21] Maxwell PH, Wiesener MS, Chang GW, Clifford SC, Vaux EC, Cockman ME, Wykoff CC, Pugh CW, Maher ER, and Ratcliffe PJ (1999). The tumour suppressor protein VHL targets hypoxia-inducible factors for oxygen-dependent proteolysis. *Nature* **399**, 271–275.

[22] Salceda S and Caro J (1997). Hypoxia-inducible factor 1alpha (HIF-1alpha) protein is rapidly degraded by the ubiquitin-proteasome system under normoxic conditions. Its stabilization by hypoxia depends on redox-induced changes. *J Biol Chem* **272**, 22642–22647.

[23] Fukuda R, Zhang H, Kim JW, Shimoda L, Dang CV, and Semenza GL (2007). HIF-1 regulates cytochrome oxidase subunits to optimize efficiency of respiration in hypoxic cells. *Cell* **129**, 111–122.

[24] Semenza GL, Jiang BH, Leung SW, Passantino R, Concordet JP, Maire P, and Giallongo A (1996). Hypoxia response elements in the aldolase A, enolase 1, and lactate dehydrogenase A gene promoters contain essential binding sites for hypoxia-inducible factor 1. *J Biol Chem* **271**, 32529–32537.

[25] Blouw B, Song H, Tihan T, Bosze J, Ferrara N, Gerber HP, Johnson RS, and Bergers G (2003). The hypoxic response of tumors is dependent on their microenvironment. *Cancer Cell* **4**, 133–146.

[26] Krishnamachary B, Berg-Dixon S, Kelly B, Agani F, Feldser D, Ferreira G, Iyer N, LaRusch J, Pak B, Taghavi P, et al. (2003). Regulation of colon carcinoma cell invasion by hypoxia-inducible factor 1. *Cancer Res* **63**, 1138–1143.

[27] Kim J, Yu W, Kovalski K, and Ossowski L (1998). Requirement for specific proteases in cancer cell intravasation as revealed by a novel semiquantitative PCR-based assay. *Cell* **94**, 353–362.

[28] Quigley JP and Armstrong PB (1998). Tumor cell intravasation alu-cidated: the chick embryo opens the window. *Cell* **94**, 281–284.

[29] Dong Z, Saliganan AD, Meng H, Nabha SM, Sabbota AL, Sheng S, Bonfil RD, and Cher ML (2008). Prostate cancer cell–derived urokinase-type plasminogen activator contributes to intraosseous tumor growth and bone turnover. *Neoplasia* **10**, 439–449.

[30] Blasi F and Carmeliet P (2002). uPAR: a versatile signalling orchestrator. *Nat Rev Mol Cell Biol* **3**, 932–943.

[31] Stoppelli MP, Corti A, Soffientini A, Cassani G, Blasi F, and Assoian RK (1985). Differentiation-enhanced binding of the amino-terminal fragment of human urokinase plasminogen activator to a specific receptor on U937 monocytes. *Proc Natl Acad Sci USA* **82**, 4939–4943.

[32] Wei Y, Lukashev M, Simon DI, Bodary SC, Rosenberg S, Doyle MV, and Chapman HA (1996). Regulation of integrin function by the urokinase receptor. *Science* **273**, 1551–1555.
[33] Reuning U, Magdolen V, Wilhelm O, Fischer K, Lutz V, Graeff H, and Schmitt M (1998). Multifunctional potential of the plasminogen activation system in tumor invasion and metastasis (review). *Int J Oncol* **13**, 893–906.
[34] Farias-Eisner R, Vician L, Silver A, Reddy S, Rabbani SA, and Herschman HR (2000). The urokinase plasminogen activator receptor (UPAR) is preferentially induced by nerve growth factor in PC12 pheochromocytoma cells and is required for NGF-driven differentiation. *J Neurosci* **20**, 230–239.
[35] Giancotti FG and Ruoslahti E (1999). Integrin signaling. *Science* **285**, 1028–1032.
[36] Soravia E, Grebe A, De Luca P, Helin K, Suh TT, Degen JL, and Blasi F (1995). A conserved TATA-less proximal promoter drives basal transcription from the urokinase-type plasminogen activator receptor gene. *Blood* **86**, 624–635.
[37] Cantero D, Friess H, Deflorin J, Zimmermann A, Brundler MA, Riesle E, Korc M, and Buchler MW (1997). Enhanced expression of urokinase plasminogen activator and its receptor in pancreatic carcinoma. *Br J Cancer* **75**, 388–395.
[38] Wood SM, Gleadle JM, Pugh CW, Hankinson O, and Ratcliffe PJ (1996). The role of the aryl hydrocarbon receptor nuclear translocator (ARNT) in hypoxic induction of gene expression. Studies in ARNT-deficient cells. *J Biol Chem* **271**, 15117–15123.
[39] Schneider M, Buchler P, Giese N, Giese T, Wilting J, Buchler MW, and Friess H (2006). Role of lymphangiogenesis and lymphangiogenic factors during pancreatic cancer progression and lymphatic spread. *Int J Oncol* **28**, 883–890.
[40] Buchler P, Reber HA, Roth MM, Shiroishi M, Friess H, and Hines OJ (2007). Target therapy using a small molecule inhibitor against angiogenic receptors in pancreatic cancer. *Neoplasia* **9**, 119–127.
[41] Nicoletti I, Migliorati G, Pagliacci MC, Grignani F, and Riccardi C (1991). A rapid and simple method for measuring thymocyte apoptosis by propidium iodide staining and flow cytometry. *J Immunol Methods* **139**, 271–279.
[42] Buchler P, Gukovskaya AS, Mouria M, Buchler MC, Buchler MW, Friess H, Pandol SJ, Reber HA, and Hines OJ (2003). Prevention of metastatic pancreatic cancer growth *in vivo* by induction of apoptosis with genistein, a naturally occurring isoflavonoid. *Pancreas* **26**, 264–273.
[43] Greenberg NM, Warren RA, Kilburn DG, and Miller RC Jr (1987). Regulation, initiation, and termination of the *cenA* and *cex* transcripts of *Cellulomonas fimi*. *J Bacteriol* **169**, 646–653.
[44] Janknecht R and Hunter T (1997). Activation of the Sap-1a transcription factor by the c-Jun N-terminal kinase (JNK) mitogen-activated protein kinase. *J Biol Chem* **272**, 4219–4224.
[45] Levy AP, Levy NS, and Goldberg MA (1996). Post-transcriptional regulation of vascular endothelial growth factor by hypoxia. *J Biol Chem* **271**, 2746–2753.
[46] Gnarra JR, Zhou S, Merrill MJ, Wagner JR, Krumm A, Papavassiliou E, Oldfield EH, Klausner RD, and Linehan WM (1996). Post-transcriptional regulation of vascular endothelial growth factor mRNA by the product of the VHL tumor suppressor gene. *Proc Natl Acad Sci USA* **93**, 10589–10594.
[47] Fink T, Kazlauskas A, Poellinger L, Ebbesen P, and Zachar V (2002). Identification of a tightly regulated hypoxia-response element in the promoter of human plasminogen activator inhibitor-1. *Blood* **99**, 2077–2083.
[48] Kvietikova I, Wenger RH, Marti HH, and Gassmann M (1997). The hypoxia-inducible factor-1 DNA recognition site is cAMP-responsive. *Kidney Int* **51**, 564–566.
[49] Buchler P, Reber HA, Buchler MW, Friess H, Lavey RS, and Hines OJ (2004). Antiangiogenic activity of genistein in pancreatic carcinoma cells is mediated by the inhibition of hypoxia-inducible factor-1 and the down-regulation of VEGF gene expression. *Cancer* **100**, 201–210.
[50] Vaupel P and Mayer A (2007). Hypoxia in cancer: significance and impact on clinical outcome. *Cancer Metastasis Rev* **26**, 225–239.
[51] Hockel M and Vaupel P (2001). Tumor hypoxia: definitions and current clinical, biologic, and molecular aspects. *J Natl Cancer Inst* **93**, 266–276.
[52] Reyes H, Reisz-Porszasz S, and Hankinson O (1992). Identification of the Ah receptor nuclear translocator protein (Arnt) as a component of the DNA binding form of the Ah receptor. *Science* **256**, 1193–1195.
[53] Hoffman EC, Reyes H, Chu FF, Sander F, Conley LH, Brooks BA, and Hankinson O (1991). Cloning of a factor required for activity of the Ah (dioxin) receptor. *Science* **252**, 954–958.
[54] Yoon SY, Lee YJ, Seo JH, Sung HJ, Park KH, Choi IK, Kim SJ, Oh SC, Choi CW, Kim BS, et al. (2006). uPAR expression under hypoxic conditions depends on iNOS modulated ERK phosphorylation in the MDA-MB-231 breast carcinoma cell line. *Cell Res* **16**, 75–81.
[55] Yamano M, Fujii H, Takagaki T, Kadowaki N, Watanabe H, and Shirai T (2000). Genetic progression and divergence in pancreatic carcinoma. *Am J Pathol* **156**, 2123–2133.
[56] Hruban RH, Wilentz RE, and Kern SE (2000). Genetic progression in the pancreatic ducts. *Am J Pathol* **156**, 1821–1825.
[57] Semenza GL, Artemov D, Bedi A, Bhujwalla Z, Chiles K, Feldser D, Laughner E, Ravi R, Simons J, Taghavi P, et al. (2001). 'The metabolism of tumours': 70 years later. *Novartis Found Symp* **240**, 251–260.
[58] Lal A, Peters H, St Croix B, Haroon ZA, Dewhirst MW, Strausberg RL, Kaanders JH, van der Kogel AJ, and Riggins GJ (2001). Transcriptional response to hypoxia in human tumors. *J Natl Cancer Inst* **93**, 1337–1343.
[59] Koong AC, Denko NC, Hudson KM, Schindler C, Swiersz L, Koch C, Evans S, Ibrahim H, Le QT, Terris DJ, et al. (2000). Candidate genes for the hypoxic tumor phenotype. *Cancer Res* **60**, 883–887.
[60] Kietzmann T, Roth U, and Jungermann K (1999). Induction of the plasminogen activator inhibitor-1 gene expression by mild hypoxia via a hypoxia response element binding the hypoxia-inducible factor-1 in rat hepatocytes. *Blood* **94**, 4177–4185.
[61] Uchiyama T, Kurabayashi M, Ohyama Y, Utsugi T, Akuzawa N, Sato M, Tomono S, Kawazu S, and Nagai R (2000). Hypoxia induces transcription of the plasminogen activator inhibitor-1 gene through genistein-sensitive tyrosine kinase pathways in vascular endothelial cells. *Arterioscler Thromb Vasc Biol* **20**, 1155–1161.
[62] Wenger RH, Stiehl DP, and Camenisch G (2005). Integration of oxygen signaling at the consensus HRE. *Sci STKE* **2005**, re12.
[63] Brahimi-Horn C and Pouyssegur J (2006). The role of the hypoxia-inducible factor in tumor metabolism growth and invasion. *Bull Cancer* **93**, E73–E80.
[64] Pouyssegur J, Dayan F, and Mazure NM (2006). Hypoxia signalling in cancer and approaches to enforce tumour regression. *Nature* **441**, 437–443.

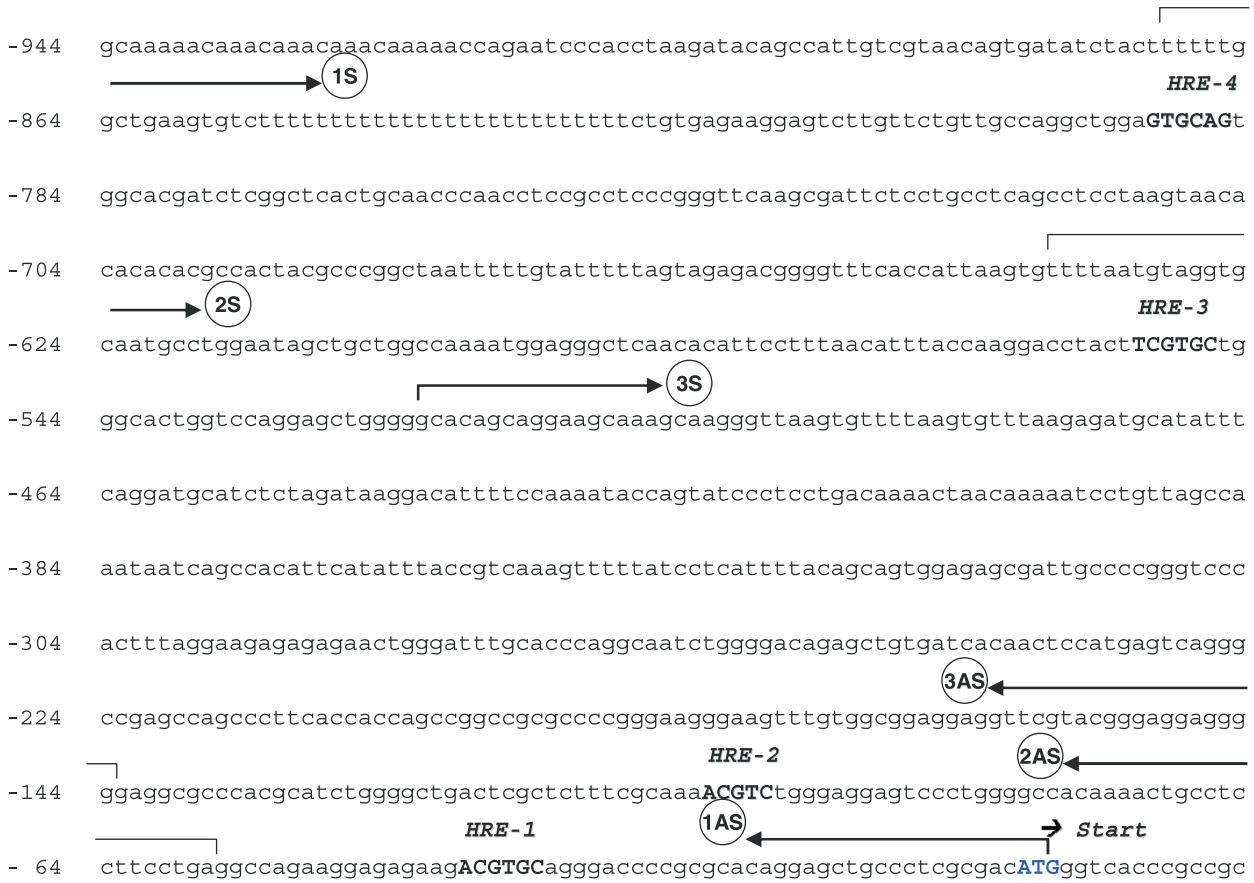

Figure W1. Sequence of the human uPAR promoter (S78532). A gene bank search was performed for hypoxia response elements within the uPAR promoter. Four putative HREs (5′-RCGTGC-3′) were identified in the uPAR promoter (NCBI Accession No. S78532). The detailed sequence, with HRE and the translation initiation site (ATG with arrow), is indicated; bold sequences indicate putative HREs. The first HRE-1 (−34 to −39), the second HRE-2 (−98 to −102), and the third HRE-3 (−547 to −552) are located on the sense strand; the fourth HRE-4 (−786 to −790) is located on the antisense strand. Sense primers used for creating deletion mutants are indicated: 1 sense (1S); 2 sense (2S); and 3 sense (3S). Reverse primers were as follows: 1 antisense (1AS); 2 antisense (2AS); and 3 antisense (3AS). The first 944 bp of the promoter sequence are shown.

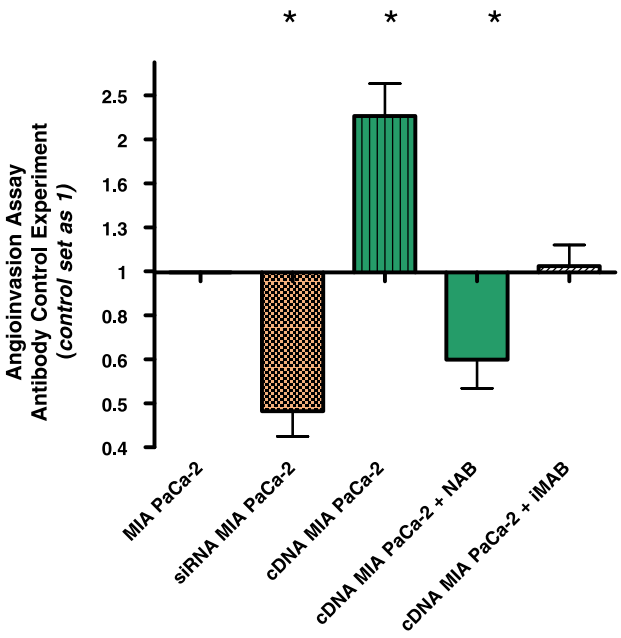

Figure W2. Angioinvasion is dependent upon uPAR expression *in vivo*. A total of 1×10^6 human cancer cells were inoculated on 10 CAMs of chicken embryos. Three days later, the lower CAMs were excised, and genomic DNA was isolated and tested for human Alu sequences (see Materials and Methods section). Inhibition of *uPAR* gene expression by siRNA resulted in reduced angioinvasion, whereas recombinant overexpression of *uPAR* increased tumor cell invasion. This increase was reducible by the addition of 40 mg/ml neutralizing uPAR antibody (NAB) biut was unchanged on the addition of an equal amount of an unspecific isotype matched antibody (IMAB). $*P < .05$ compared with untreated control cells.

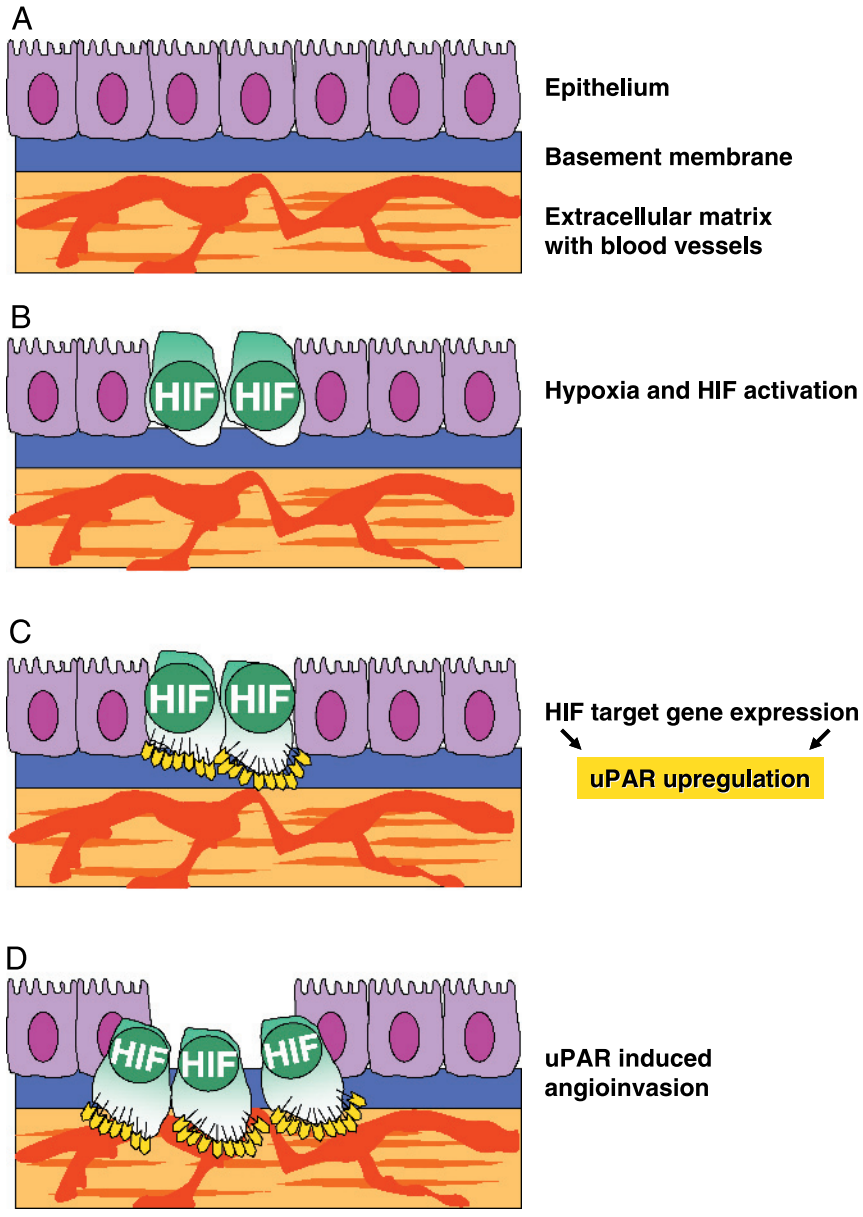

Figure W3. Hypoxia-induced angioinvasiobn by upregulation of *uPAR* expression through HIF-1 activation. Cell migration from the primary tumor and invasion into adjacent blood vessels is a multistep process leading to metastasis in carcinomas. Invasion requires a proteolytic modification of the extracellular matrix and tumor cell migration. Hypoxia-inducible factor activates proteolysis by the induction of uPAR. (A) Normal epithelial cells are located on a basement membrane with close contact to the ECM. Under low-oxygen conditions (hypoxia), HIF-1 is active (B) and induces the expression of uPAR (C). This pathway might account for increased angioinvasion (D), which represents the central and rate-limiting step of the metastatic cascade.